Scanning-tunneling-microscopy observation of K-induced reconstructions on Au(110)

J. V. Barth,* R. Schuster, J. Wintterlin, R. J. Behm,† and G. Ertl
Fritz-Haber-Institut der Max-Planck-Gesellschaft, Faradayweg 4-6, D-14195 Berlin (Dahlem), Germany
(Received 29 April 1994)

The K-induced reconstructions of the Au(110) surface at coverages up to 0.5 ML and various deposition and annealing temperatures were investigated by scanning tunneling microscopy. At very low coverages (<0.1 ML) the K atoms stabilize missing-row-type structures with deep (1×3) channels. A (1×5) structure that consists of alternating (1×3) and (1×2) missing-row furrows is formed at $\theta_K \approx 0.05$ ML, and a (1×3) phase appears at $\theta_K \approx 0.08$ ML. A (1×2) missing-row structure, identical to that of the clean surface, is found in the coverage range between 0.15 and 0.25 ML. At coverages beyond 0.25 ML the K atoms disrupt the densely packed Au atomic rows of the surface, and highly anisotropic elements of a $c(2\times2)$ structure are formed. It is shown that, in agreement with previous studies, the $c(2\times2)$ structure consists of a mixed K-Au surface layer.

I. INTRODUCTION

The clean (110) surfaces of the 5*d* fcc metals Au and Pt exhibit (1×2) missing-row reconstructions where every second densely packed row of atoms along the $[1\bar{1}0]$ direction is absent.[1–5] It was suggested that this reconstruction is stabilized by the (111) microfacets which form the reconstruction channels.[6,7] First-principles pseudopotential density-functional calculations for the Au(110) surface indicate that the surface charge plays a crucial role for the stability of the missing-row configuration on this surface.[8] This is supported by the observation that reconstructions of the same type can be induced on the (110) surfaces of the 3*d* and 4*d* fcc metals Ni, Cu, Pd, and Ag by adsorption of small amounts of alkali metals.[9,10] Without adsorbates these surfaces are not reconstructed. The alkali-metal-induced missing-row reconstructions were attributed to an increase of the surface *sp* electron density due to electron donation from the electropositive adsorbate to the substrate surface.[8,11] Alternatively these reconstructions were attributed to the gain in adsorption energy of the adsorbed atoms in the missing-row substrate troughs.[12]

The missing-row reconstructed Au(11)) surface is also highly reactive towards adsorbed alkali-metal atoms. Using low-energy electron diffraction (LEED), it was shown that small amounts of K or Cs induce a (1×5) and a (1×3) structure ($\theta<0.1$ ML).[13,14] For the Cs/Au(110)(1×3) structure a medium-energy-ion-scattering (MEIS) study revealed that the structure of the surface corresponds to a missing-row reconstruction where two adjacent atomic rows of the first and in addition a row of atoms of the second layer are missing.[14] In recent *in situ* x-ray-scattering studies of the Au(110) electrode surface in salt solutions, a similar (1×3) structure was identified at sufficiently negative potentials.[15] To explain this result, it was proposed that this reconstruction is induced by negative surface charge.[15] In the case of K/Au(110) the nature of the (1×5) and (1×3) phases has not been clarified yet, and it was found that intermediate K coverages ($0.15<\theta_K<0.30$ ML) stabilize the (1×2) reconstruction.[13] At even higher K coverages the surface structure changes again, and a $c(2\times2)$ superstructure with a saturation coverage of 0.5 ML was observed by LEED.[13,16] For the K/Au(110) $c(2\times2)$ phase first-principles total-energy calculations were performed.[17] It was shown that the most stable $c(2\times2)$ structure is achieved by a mixed K-Au surface layer where both K and Au atoms form a $c(2\times2)$ pattern and atoms of one species are surrounded by four atoms of the other species (shifted-row model). A MEIS analysis of the K/Au(110)$c(2\times2)$ structure confirmed this prediction.[18] This structure is formed only on the Au(110) substrate. For other fcc transition metals no intermediate phases were observed between the missing-row reconstructions at low alkali-metal coverages and the formation of alkali-metal multilayers. This peculiarity suggests a correlation with the tendency of Au to form alloys with the alkali metals.[17] As with the alkali-metal-induced reconstructions on other fcc (110) surfaces[9] the K- and Cs-induced reconstructions on Ac(110) require thermal activation.[13,14,18]

In this paper we report results of a scanning-tunneling-microscopy (STM) investigation on the interaction of Au(110) with adsorbed K atoms in the coverage range up to 0.5 ML. We show that for K coverages below 0.15 ML a reordering of the surface takes place where missing-row-type structures with deep furrows are formed. For intermediate coverages (0.15–0.25 ML) STM images are obtained which resolve a (1×2) missing-row structure of the substrate. For coverages in excess of 0.25 ML the formation of the $c(2\times2)$ phase was observed, where K atoms disrupt the densely packed Au atomic rows. Antiphase domain boundaries (APDB's) of the (1×2) missing-row reconstruction and elements of the $c(2\times2)$ shifted-row phase evolve on the surface. The $c(2\times2)$ phase exhibits a unique nucleation and growth behavior, which is related to the repulsive interaction of the K atoms adsorbed in (1×2) missing-row troughs and to the anisotropy of the Au(110) substrate.

0163-1829/95/51(7)/4402(13)/$06.00

II. EXPERIMENT

The experiments were performed in an ultrahigh-vacuum chamber with a base pressure of 1×10^{-10} Torr, equipped with facilities for sample preparation, surface characterization [LEED and Auger electron spectroscopy (AES) with a cylindrical mirror analyzer], and a pocket-size STM.[19,20] The Au(110) sample was prepared by cycles of Ar^+ sputtering (2 μA/cm^2, 700 eV, 30 min) and thermal annealing at 1000 K until no contamination could be detected by AES, and the LEED pattern showed sharp diffraction beams of the (1×2) reconstruction.

Potassium atoms were evaporated from a commercial getter source (SAES Getters SpA, Milano, Italy). To elucidate thermal effects the Au sample was either heated to $T\approx450$ K or held at room temperature during deposition. The potassium coverage was determined by AES from the intensity of the 252-eV LMM transition of K. Since this peak overlaps with the NVV transition of Au at 255 eV, the intensity of the 252-eV peak was corrected for the substrate intensity by a deconvolution method described in an earlier paper.[13] The absolute coverage was calibrated using the Auger signal from the saturated $c(2\times2)$ structure which corresponds to a K coverage of 0.5 ML (Refs. 13, and 18). (1 ML corresponds to one K atom per surface Au atom on the unreconstructed (1×1) Au(110) surface.)

For STM imaging an electrochemically etched tungsten tip was used which was cleaned prior to the experiments by field desorption in front of a Au foil. The STM data were recorded in the constant-current mode, with typical tunneling currents between 0.3 and 3 nA and tunnel voltages of −500 to −1000 mV (tip negatively biased). STM images consist of about 400×400 data points and are usually displayed in top-view, gray-scale representations where darker areas correspond to lower levels. No filtering procedures were applied to the data presented here.

III. RESULTS

In all STM images shown here the adsorbed K atoms are not directly visible. It is hence just the K-induced restructuring of the Au surface which is reflected by the images. The transparency of the K atoms, which was similarly observed for K-induced reconstructions on the Cu(110) surface,[10] is discussed in a separate paper.[21] The differences in height are given with respect to the plane which is defined by the maxima of densely packed Au rows in the individual terraces. The data presented here show typical structures which evolve upon adsorption of K. The images were usually selected in such a way as to display relatively large terraces in order to show these structures clearly; the same structures were observed, however, on smaller terraces also.

A. K-induced missing-row type structures

For very small K coverages a (1×5) LEED structure is formed upon annealing the Au(110) crystal.[13] Figure 1(a) shows a STM image of the Au(110) surface covered with ≈0.05 ML K. Domains of a (1×5) phase are resolved, which consist of a sequence of alternating (1×2) and (1×3) troughs. These domains are separated by single (1×3) furrows. The corrugation amplitude of the (1×2) and (1×3) elements amounts to about 0.6 and 1.2 Å, respectively [cf. Fig. 1(b)]. These values are typical also for the (1×2) missing-row troughs and the (1×3) missing-row domain boundaries on the clean surface.[22] Therefore the model depicted in Fig. 1(c) is suggested for the K-induced (1×5) structure. A (1×5) element consists of a (1×2) next to a (1×3) missing-row trough. In the (1×2) trough one Au atomic row is missing, similarly to the clean reconstructed surface. In the deep (1×3) trough two atomic Au rows of the first and one of the

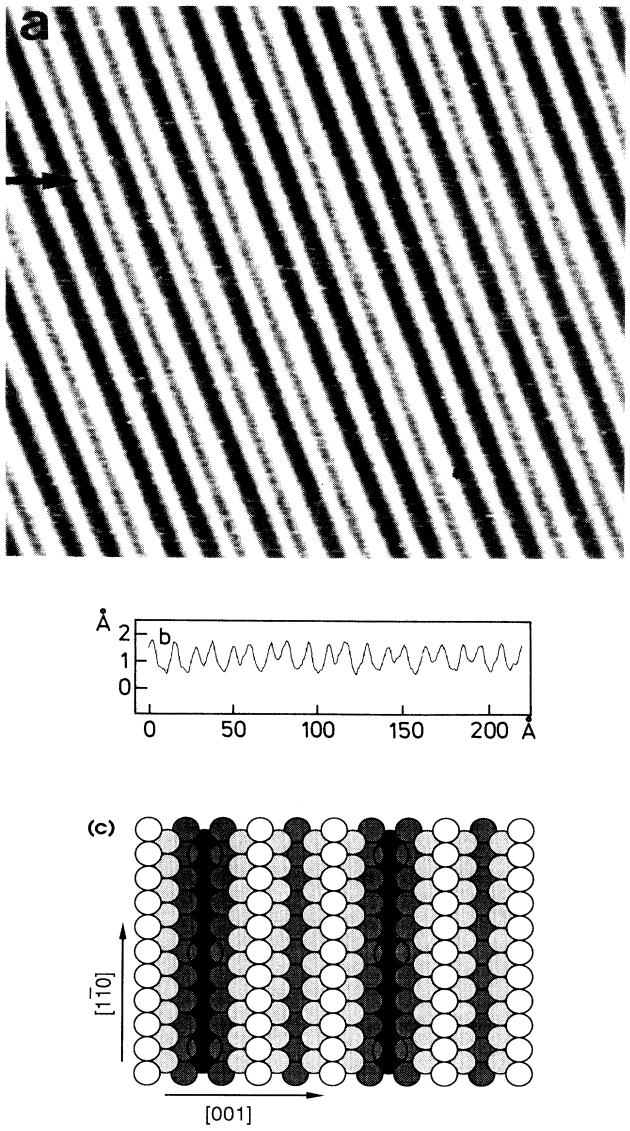

FIG. 1. (a) STM image of the Au(110) surface for $\theta_K\approx0.05$ ML (annealed to 1000 K). Domains of the K-induced (1×5) reconstruction separated by single (1×3) elements are resolved (220×220 Å^2); (b) contour line along the marked direction in (a) (arrow); (c) model of the K-induced (1×5) reconstruction; small circles correspond to Au atoms, lower-lying atoms are darker colored, and large open circles correspond to adsorbed K atoms.

second layer are absent.

At slightly higher K coverages ($\theta_K \approx 0.1$ ML) a regular (1×3) reconstruction is formed on the surface.[13] A STM image of the K-induced (1×3) phase for a coverage of ≈0.08 ML is shown in Fig. 2(a). The image demonstrates that the step-terrace topography of the (1×3) reconstructed surface closely resembles that of the clean surface.[22,23] The steps along the densely packed [1$\bar{1}$0] direction are usually straight, whereas those along [001] are irregular. Almost on the entire surface well-ordered (1×3) areas exist which are only occasionally interrupted by single (1×2) furrows. The corrugation amplitude of the (1×3) phase amounts to ≈1 Å in this measurement [cf. Fig. 2(b)]. Again, this value is typical also for the corrugation of the (1×3) domain boundary channels on the clean surface. In accordance with the Cs-induced Au(110) (1×3) reconstruction,[14] we interpret the K-induced (1×3) phase on Au(110) as a missing-row-type structure with deep (1×3) furrows, where Au atoms of the first and second layers are absent. This is illustrated by the model in Figs. 2(c) and 2(d).

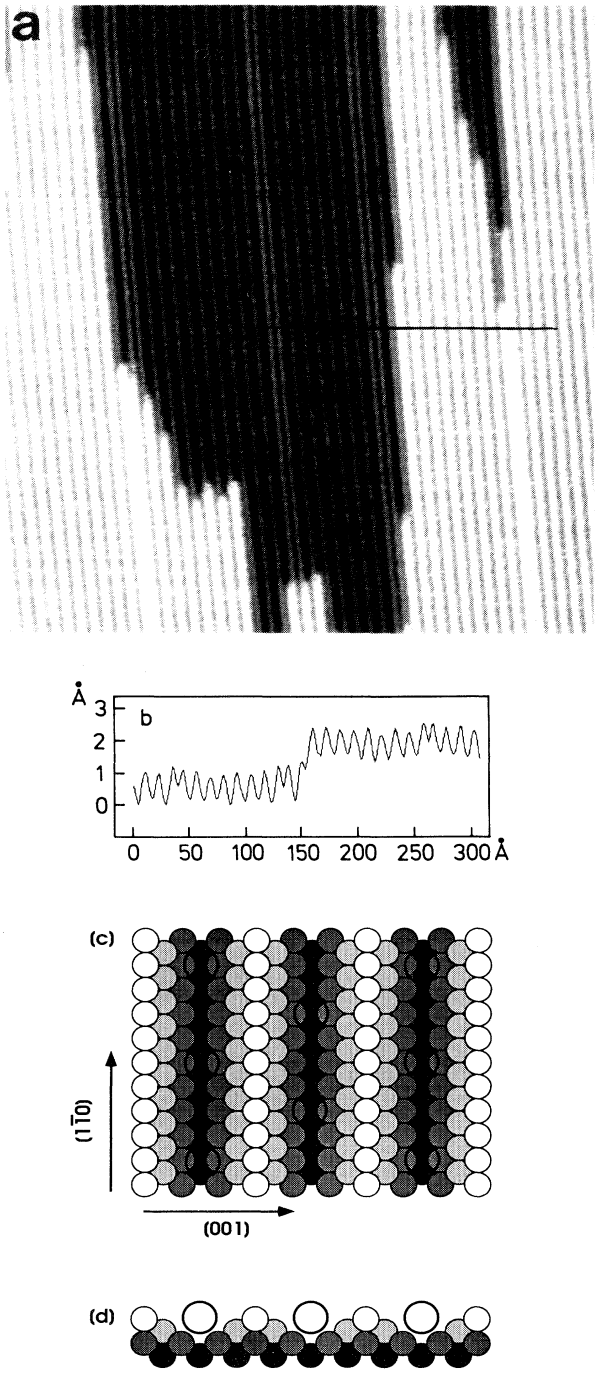

FIG. 2. (a) STM image of the Au(110) surface for $\theta_K \approx 0.08$ ML (annealed to 950 K): K-induced (1×3) reconstruction with single (1×2) troughs (610×510 Å^2); (b) STM contour along the marked line in (a); (c) model of the K-induced (1×3) phase on Au(110), top view; (d) side view.

An interesting detail in Fig. 2(a) is the structure of the monoatomic steps which run parallel to the reconstruction. The STM contour line in Fig. 2(b) demonstrates that the step edge does not correspond to a single large (111) facet but to two smaller (111) facets which are separated by a (1×2) furrow. This holds similarly for all other steps on the surface. As the surface had been annealed to 950 K, kinetic restrictions can be ruled out to explain this finding. We conclude that, for Au(110) covered with small amounts of K, there is no driving force to form (111) microfacets larger than those in the (1×3) reconstruction. This is in accordance with the observation that the K/Au(110)(1×5) phase consists of (1×2) and (1×3) channels rather than of deep (1×5) missing-row furrows.

The transition from the (1×2) to a well-ordered (1×3) missing-row structure requires long-range mass transport of Au atoms on the surface. The (1×3) reconstruction has the same average density as a (1×1) structure (spread over two layers), whereas the density of Au atoms of the (1×2) reconstruction amounts to 0.5 ML. In order to gain insight into the mechanism of the (1×2)-(1×3) transformation, ≈0.08 ML K were evaporated onto the sample at room temperature. At this temperature a regular (1×3) phase cannot be generated. Immediately after the adsorption, in addition to the (1×2) LEED spots, stripes along [01] were observed between the (1×1) spots, indicating substantial surface disorder along the [001] direction. The STM images reproduced in Fig. 3 were recorded about 30 min after K adsorption. The image shown in Fig. 3(a) reveals that small terraces (width along [1$\bar{1}$0] smaller than ≈200 Å) exhibit a (1×3) structure, whereas the large terrace in the upper right of the image is still (1×2) reconstructed. The (1×2)-(1×3) transition is apparently faster on smaller terraces. This can be rationalized in terms of a mechanism which is connected with the atomic steps. By removal of missing-row Au atoms from the steps (or by deposition of surplus atoms at the steps) the system can compensate for the change in density during the (1×2)-(1×3) transition. The (1×2-(1×3) transition on larger terraces is not so easily achieved and follows a different mechanism. In Fig. 3(b) a part of the surface shown in Fig. 3(a), which was imaged about 5 min later, is reproduced. Between the two measurements a

structural modification of the surface occurred. On the (1×2) terrace in Fig. 3(b) a single protrusion with a height of ≈1.2 Å and a length of ≈300 Å is resolved which is oriented along the (1×2) reconstruction. Protrusions of this type will be called elevated rows in the following. Running parallel to this protrusion a single trough, ≈1 Å deep, is resolved [for comparison, the corrugation amplitude of the (1×2) reconstruction amounts to ≈0.5Å in this measurement]. These structures are considered as a first step of the transition of the (1×2) to the (1×3) missing-row structure on a (1×2) terrace, as illustrated in the model in Fig. 3. The formation of the elevated row next to the trough is accomplished by shifting two densely packed atomic Au rows by one lattice constant in [001] direction. This leads to a deep (1×3) furrow and a single Au atomic row above the level of the (1×2) reconstruction.

For K coverages above ≈0.10 ML the (1×3) reconstruction does not represent the thermodynamic equilibrium phase and for $\theta_K > 0.15$ ML the adsorbed K atoms stabilize the (1×2) reconstruction.[13] After adsorption of 0.10 ML K at $T=450$ K a LEED pattern with streaky (1×2) and (1×3) reconstruction spots was observed. A STM image of the corresponding surface structure is shown in Fig. 4. The image shows that the surface is mostly (1×2) reconstructed with additional elevated rows. Also, 1.5-Å-deep (1×5) channels are resolved. By comparison, the depth of the (1×3) furrows in this measurement amounts to 0.8 Å. These (1×5) troughs are clearly different from the (1×5) structure which was found at lower coverages (cf. Fig. 1). Presumably, they are missing-row furrows where Au atoms from several layers are removed.

With increasing K coverage the fraction of the (1×2) surface area increases, and, after adsorption of ≈0.13 ML K at $T \approx 450$ K, only the (1×2) reconstruction spots

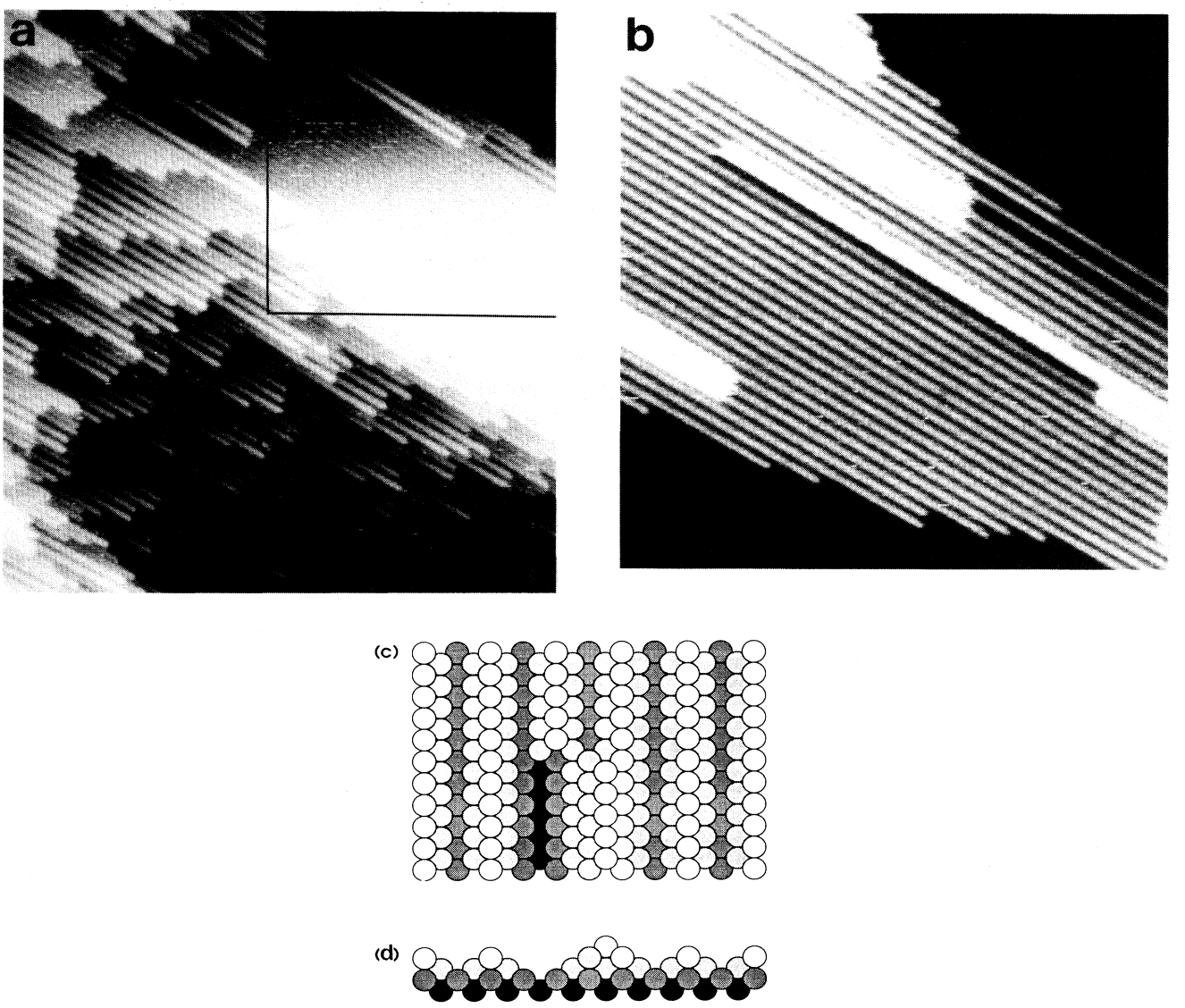

FIG. 3. Au(110) surface ≈30 min after the adsorption of ≈0.08 ML K at room temperature (700×700 Å^2); (b) detail from the area marked in (a), recorded ≈5 min later (370×370 Å^2). Model of the elevated row: (c) top view; (d) side view.

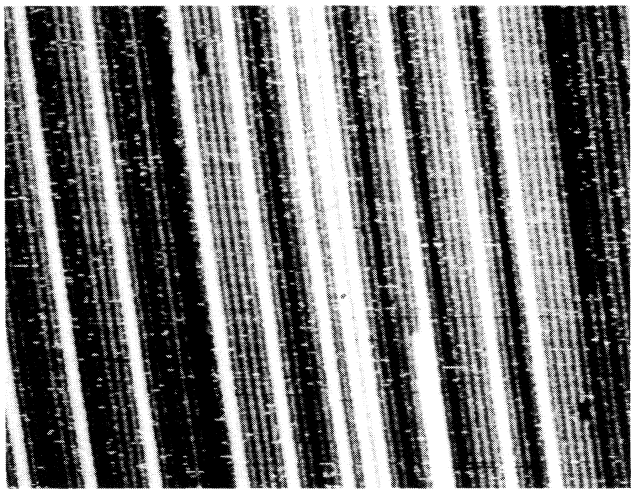

FIG. 4. Au(110) for $\theta_K \approx 0.10$ ML adsorbed at $T \approx 450$ K (570×450 Å^2).

were observed in the LEED pattern. Corresponding STM images of the surface demonstrate that the (1×2) reconstruction dominates on the surface. Deep troughs that are attributed to several missing atomic Au rows and protrusions formed by additional atomic Au rows, however, still exist in the terraces.

For K coverages in the range between 0.15 and 0.25 ML the (1×2) missing-row reconstruction of the Au(110) substrate is stable, independent of the adsorption temperature.[13] STM images of such surfaces exhibit the same characteristics as those of the (1×2) reconstructed clean surface. This is illustrated by the image in Fig. 5(a), which was recorded after adsorption of 0.15 ML K at 700 K. Similar images were obtained for coverages up to 0.25 ML. At $\theta_K = 0.15$ ML the K-K distance in the missing-row furrows amounts to about 10 Å (because of the mobility of the K adatoms and their basically repulsive interaction, it can be assumed that they are uniformly distributed in the reconstruction troughs). Increasing the coverage to 0.25 ML apparently leads to a compression of the adsorbed atoms in the reconstruction troughs, whereby the average K-K distance along $[1\bar{1}0]$ reduces to 5.8 Å $= 2a$ ($a = 2.884$ Å is the next-neighbor distance of surface Au atoms in $[1\bar{1}0]$). A model for the surface at $\theta_K = 0.25$ ML is depicted in Fig. 5(b).

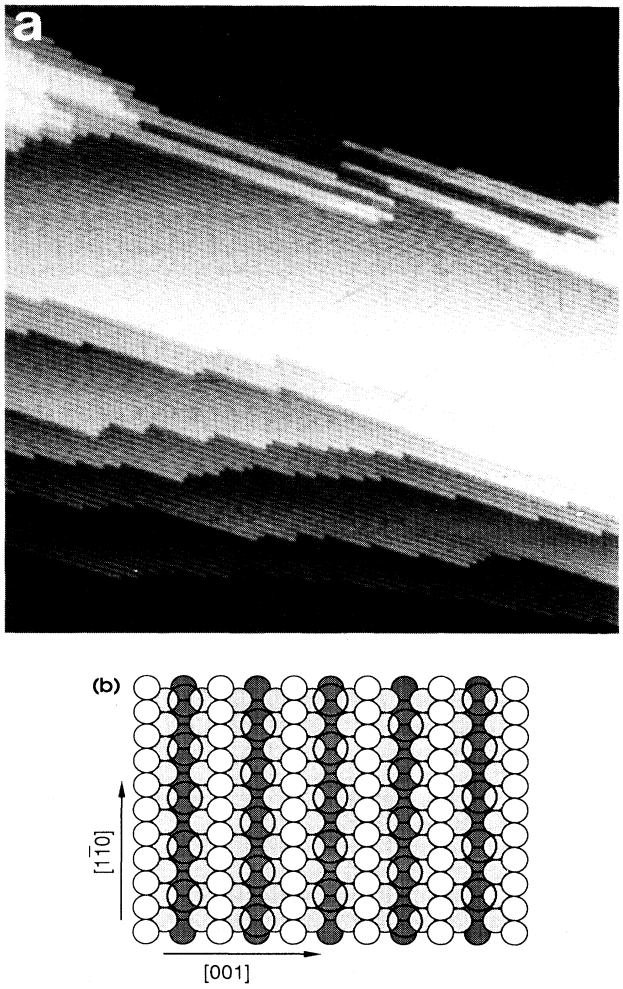

FIG. 5. Au(110)(1×2) missing-row reconstruction for $\theta_K \approx 0.15$ ML K, adsorbed at 700 K (900×900 Å^2); (b) model of the K-covered (1×2) reconstruction with $\theta_K = 0.25$ ML.

B. Formation of the K/Au(110)c(2×2) phase

For K coverages beyond ≈ 0.25 ML novel K-induced structures appear on the surface. The STM image in Fig. 6(a) demonstrates that, after adsorption of ≈ 0.25 ML K at $T \approx 450$ K, almost the entire surface is (1×2) reconstructed. Additionally, however, two bright lines are resolved which are not oriented along a low-index direction of the surface. The STM image demonstrates that these lines correspond to antiphase domain boundaries of the (1×2) reconstruction. The atomic Au rows on one side of the corrugation lines point to missing rows on the other side and vice versa. Such structures were never found on the clean Au(110) surface. For their formation Au-Au bonds of densely packed Au atomic rows must be disrupted and (1×2) areas must be shifted by one Au lattice constant along [001]. Since these APDB's were formed after the K coverage was increased beyond a critical value, they are associated with the K atoms. We assume that at these lines the density of K atoms is locally higher and that K atoms are directly bound to the Au atoms at the ends of the interrupted Au rows. A model of the K-induced APDB is given in Fig. 6(b). From this model it becomes obvious that the APDB represents a precursor to the intermixed c(2×2) phase. The four gold atoms at the ends of two pairs of interrupted atomic Au rows form half a unit cell of the c(2×2) structure (or one complete primitive cell), as indicated in the model.

The mobility of the K-induced APDB is demonstrated by the series of STM images in Fig. 7. Figure 7(a) shows an APDB which connects two defects of the missing-row/elevated-row type. The images in Figs. 7(b) and 7(c) were recorded 5 and 10 min later, respectively. In Fig.

7(b) the APDB is split into two parts which have drifted apart. The striped area in the central part of the image signals a rapid movement of the surface atoms. In Fig. 7(c) the APDB is nearly in its initial shape again. The atomic structure of the APDB is better resolved in these images. The atomic Au rows are simply interrupted. The atoms which terminate the Au rows are imaged ≈ 0.2 Å higher than those in the surrounding (1×2) areas.

For K coverages between 0.30 and 0.50 ML coexisting (1×2) and $c(2\times2)$ LEED spots were observed.[13] The intensity of the $c(2\times2)$ spots grows with increasing coverages at the expense of the (1×2) intensity. The latter spots disappear completely at $\theta_K \approx 0.50$ ML. The $c(2\times2)$ spots appear round in the coexistence regime, suggesting the formation of isotropic $c(2\times2)$ islands.[13] After the adsorption of 0.30–0.35 ML K at $T \approx 400$ K the LEED pattern shows, in addition to the $c(2\times2)$ and (1×2) spots, weak streaks along [10] and [01] which go through the $c(2\times2)$ spots. This is illustrated by the schematic LEED pattern in Fig. 8(a). A STM image of the corresponding surface structure is reproduced in Fig. 8(b). Stripes, oriented along [001], which are about 100 Å long and 10 Å wide and have corrugation amplitudes of $\simeq 0.3$ Å are visible. The average distances of these stripes along $[1\bar{1}0]$ amount to ≈ 40 Å. Across the whole surface elevated rows and (1×3) troughs with an average length of ≈ 50 Å are found, which are oriented along $[1\bar{1}0]$. The surface concentration of all these structures increases with K coverage. Their distribution is not influenced by atomic steps, and they exist equally on small and large terraces.

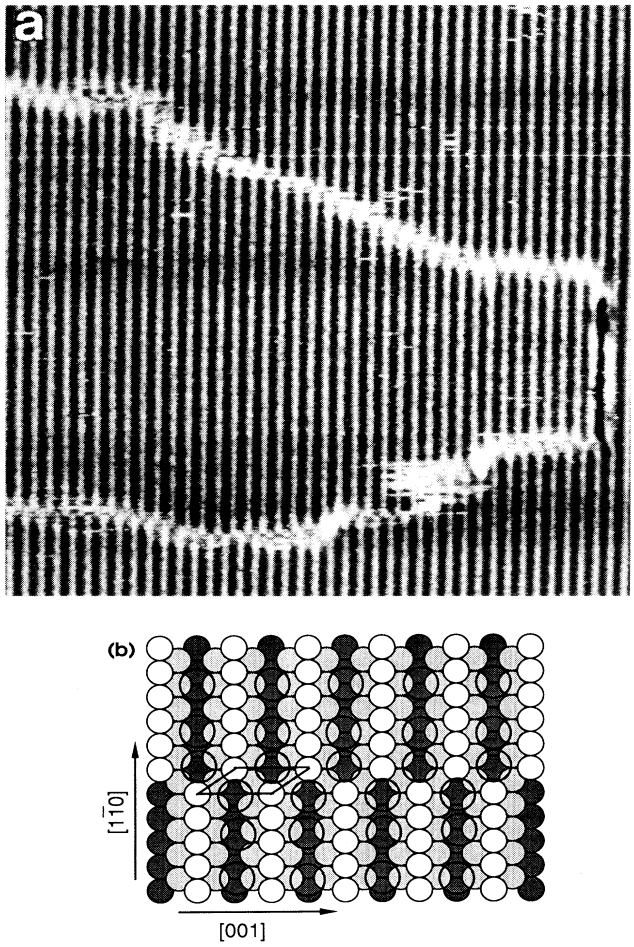

FIG. 6. Au(110) for $\theta_K \approx 0.25$ ML K, adsorbed at $T \approx 450$ K. (a) Antiphase domain boundaries of the (1×2) reconstruction (370×370 Å^2); (b) model of the K-induced antiphase domain boundary at $\theta_K \approx 0.25$ ML.

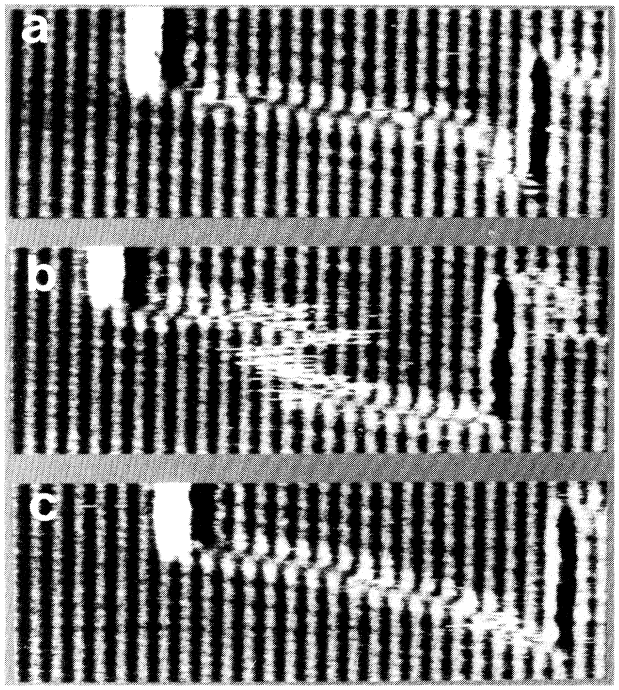

FIG. 7. Mobility of the antiphase domain boundaries for $\theta_K \approx 0.25$ ML, adsorbed at $T \approx 450$ K. The images in (b) and (c) were recorded ≈ 5 and 10 min after the image in (a), respectively (each 230×80 Å^2).

With increasing coverage of potassium the number and width of the bright [001] streaks increase. This is demonstrated in the STM image in Fig. 9(a), which was recorded on a surface with $\theta_K = 0.35$ ML. The resolution is better than in Fig. 8(b) and the (1×2) periodicity of the darker areas between the streaks is visible. [The very bright features in Fig. 9(a), which are streaks parallel to the (1×2) reconstruction, are elevated rows. Sharp cutoffs of these structures are due to sudden displacements which occurred between two scan lines while recording the STM image.] STM images of the same area, recorded some minutes later, demonstrates that the arrangement of the [001] stripes also can change. The K-induced structures are consequently mobile on the time scale of the STM experiment, similar to the APDB in Fig. 7. Figure 9(a) shows that the [001] stripes have varying widths and that these are connected with the phase relation of the (1×2) areas above and below the stripes as either in or out of phase: The narrowest stripes are APDB's, identical to that in Fig. 7, for the 9-Å wide

stripes the (1×2) areas are in phase, for the 12-Å-wide stripes they are again out of phase, and so on. The 9-Å and 12-Å stripes are the most frequent type in this figure.

Furthermore, the (1×2) areas exhibit discrete lengths in [1$\bar{1}$0]. The preferred lengths amount to 3a and 5a, i.e., to odd multiples of the nearest-neighbor (NN) distance of surface Au atoms. Sometimes the APDB's form a network where (1×2) areas with a length of 3a are interconnected [e.g., in the center left in Fig. 9(a)]. The reason for the discrete lengths of the (1×2) areas is rationalized by the models in Fig. 9. We assume that K atoms are bound directly to the ends of the interrupted atomic Au rows. Furthermore, we assume that the radius of the adsorbed K atoms amounts to ≈ 1.9 Å, similar to the radius of K atoms in the $c(2\times2)$ phase[17] or in K-Au alloys.[24,25] Then two K adatoms fit into a (1×2) trough with a length of 3a. In a trough with a length of 5a, three K atoms can be accommodated. The K coverage in the (1×2) area between the APDB's amounts to 0.25 ML, that in the stripes to 0.50 ML.

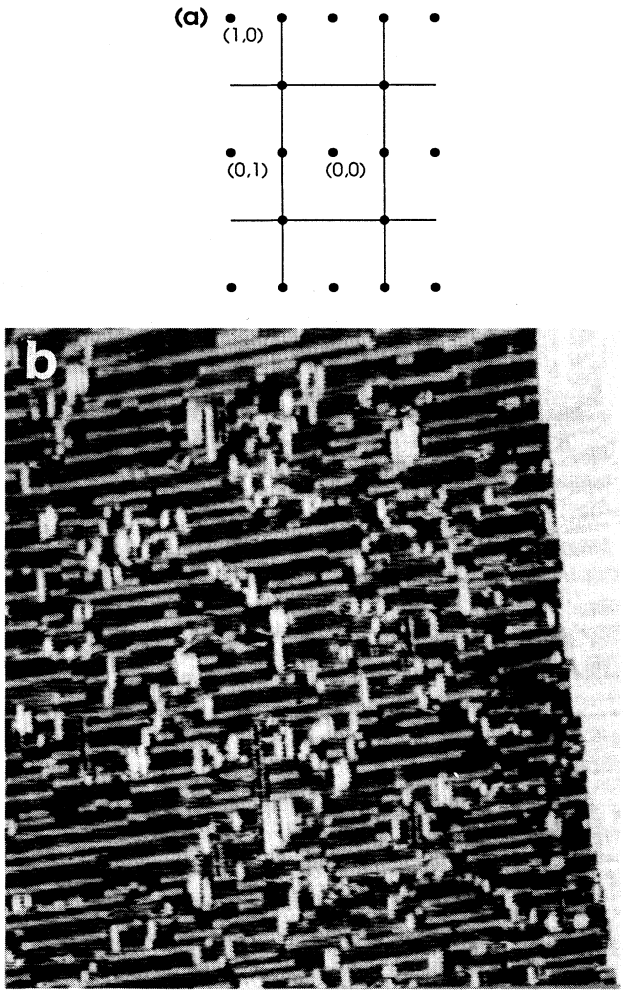

FIG. 8. (a) Schematic LEED pattern of the Au(110) surface covered with 0.30–0.35 ML, K, adsorbed at ≈400 K; (b) corresponding STM image ($\theta_K \approx 0.30$ ML; 1000×1000 Å^2).

The atomic structure of the stripes along [001] is shown in the STM image in Fig. 10(a). The atomic Au rows of the (1×2) reconstruction are interrupted by depressions (≈0.1 Å deep). Between these depressions spherical protrusions (≈0.3 Å high) are resolved which form chains along [001] with (1×2) periodicity. Together with the Au atoms at the ends of the interrupted (1×2) rows these atoms form unit cells of the $c(2\times2)$ structure. The protrusions are associated with Au atoms. Only in this way can the $c(2\times2)$ LEED spots be rationalized, which were observed prior to and after the STM experiments. Consequently, the stripes along [001] correspond to elements of the $c(2\times2)$ shifted-row structure. Thus, the theoretical predictions[17] and the MEIS results[18] for the $c(2\times2)$ phase are confirmed.

A model of a narrow $c(2\times2)$ stripe which separates two (1×2) areas which are in phase is depicted in Fig. 10(b). Similarly to the structure of the saturated $c(2\times2)$ phase,[17,18] we assume that the K atoms are bound directly to the isolated Au atoms and occupy the hole in the interrupted (1×2) reconstruction row. The K atoms at the stripes are also arranged in a $c(2\times2)$ pattern. This structure is considered as the nucleus of the $c(2\times2)$

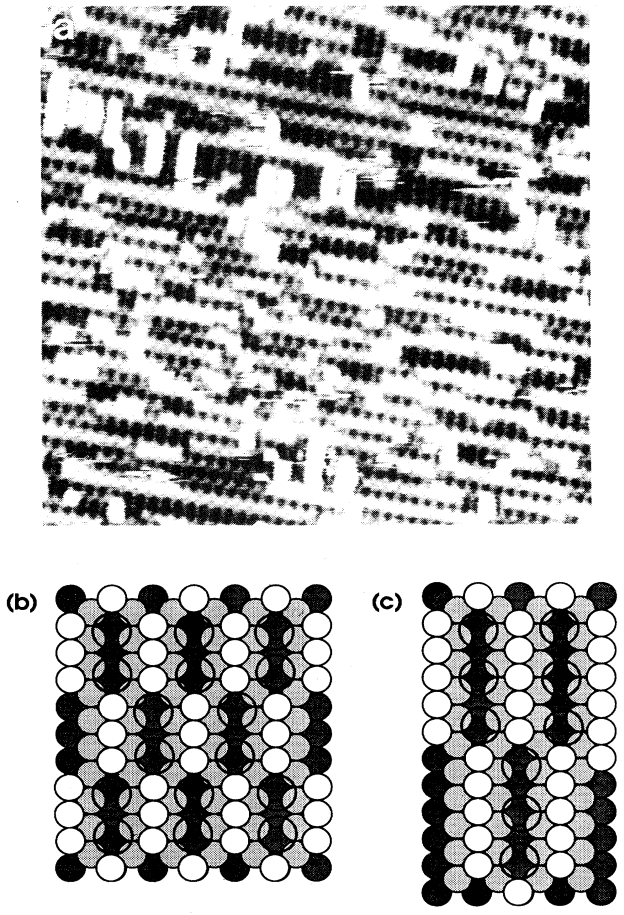

FIG. 9. (a) Au(110) for $\theta_K \approx 0.35$ ML, adsorbed at $T \approx 400$ K (350×350 Å^2). (b) K-induced antiphase domain boundaries regular network with a periodicity of 3a along [1$\bar{1}$0]; (c) three K atoms fit into a (1×2) trough with a length of 5a.

phase since it corresponds to the smallest structure where the planar coordination number of Au and K atoms with respect to each other is 4, as in a perfect $c(2\times2)$ layer. Single elements of the $c(2\times2)$ structure [i.e., an individual Au atom between two interrupted (1×2) reconstruction rows] were never observed in the STM measurements. The shortest $c(2\times2)$ stripes found consist of two or three neighboring $c(2\times2)$ unit cells. The above mentioned $\approx$12-Å-wide stripes along [001] which represent APDB's for the (1×2) areas are equivalently rationalized in the shifted-row scheme, as shown in Fig. 10(c).

The preferred widths of the (1×2) areas which separate the $c(2\times2)$ stripes amount to $3a$ and $5a$. The reason for these values is attributed to the packing of the K atoms in the (1×2) missing-row troughs, as demonstrated in the models in Figs. 9 and 10. This has important consequences for the phase relation of the $c(2\times2)$ stripes. From the symmetry of the $c(2\times2)$ structure two

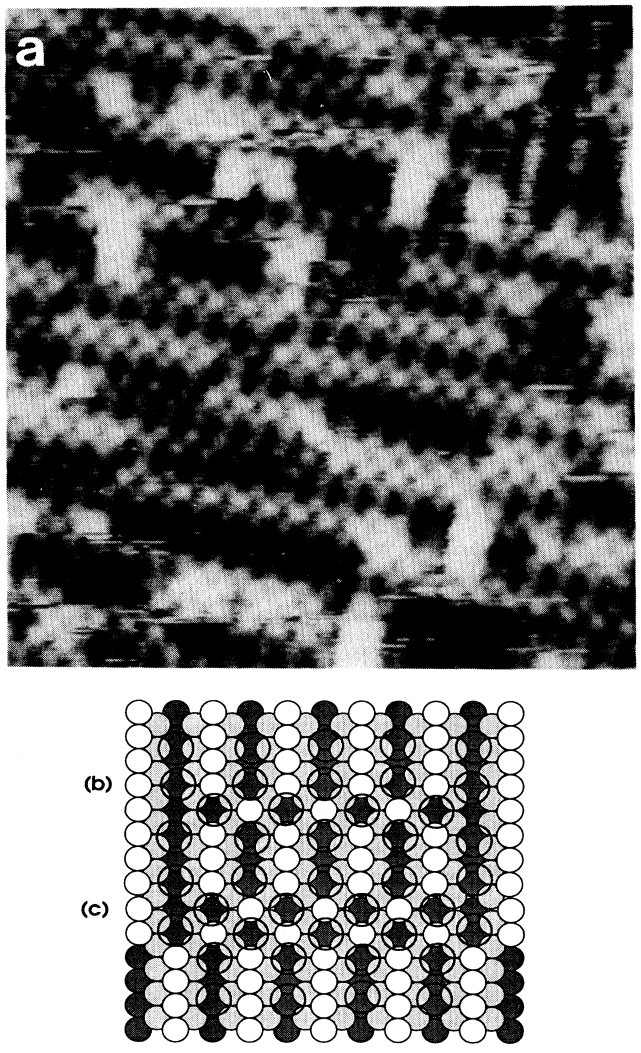

FIG. 10. (a) Atomic-resolution STM image of the K-induced structures on Au(110) for $\theta_K \approx 0.35$ ML, adsorbed at $T \approx 400$ K (170×180 Å^2); (b) model for the $c(2\times2)$ nucleus; (c) model for the $c(2\times2)$ antiphase domain boundary.

inequivalent translational domains exist. If the $c(2\times2)$ stripes were independent of each other, they would adopt both possible arrangements with the same probability, and in-phase and out-of-phase relationships would be equally likely. Because of the anisotropy of the $c(2\times2)$ islands the LEED spots should then not be round, as is actually observed. However, because the widths of the (1×2) areas between neighboring $c(2\times2)$ stripes are odd multiples of the substrate lattice constant, the $c(2\times2)$ stripes are all in phase. Consequently, neighboring $c(2\times2)$ stripes contribute by constructive interference to the $c(2\times2)$ spots in LEED and the observation of $c(2\times2)$ spots at intermediate K coverages is due to this phase relation. While the LEED observation of a coexistence of $c(2\times2)$ and (1×2) spots might be interpreted in terms of a separation of the respective surface phases into areas of sizable diameters, the STM results demonstrate that such conclusions can be misleading. The stripes in the LEED pattern along [01] at the position of the $c(2\times2)$ spots are due to the uncorrelated rows of K atoms adsorbed in the (1×2) missing-row troughs. The stripes along [10] connecting (1×2) and $c(2\times2)$ spots are related to the varying (small) widths of the (1×2) patches along $[1\bar{1}0]$.

In the models shown in Figs. 6, 9, and 10 it was assumed that the sites where $(1\times2$ Au reconstruction rows are interrupted and the sites inside the wider $c(2\times2)$ stripes are occupied by K atoms. The local K coverage of the $c(2\times2)$ areas therefore amounts to 0.5 M and, hence, is higher than the average K coverage on the surface. The increasing density of $c(2\times2)$ elements on the surface with increasing coverage and the first occurrence of the APBD's for coverages beyond 0.25 ML (cf. Fig. 6) also signal that the K atoms are inhomogeneously distributed on the surface when (1×2) and $c(2\times2)$ structures coexist. To confirm the models, we estimated the K coverages from STM images of the Au(110) surface covered with 0.30 and 0.35 ML K under the following assumptions: (i) the local density of K atoms in the $c(2\times2)$ areas is 0.5 ML; (ii) at the borders between the (1×2) and $c(2\times2)$ areas the K atoms are located directly at the ends of the interrupted Au rows; (iii) the local coverage in (1×2) areas is 0.25 ML. For simplicity, the (1×3) troughs and the elevated rows were not taken into consideration since they occupy only a small fraction of the surface area. Agreement within a K coverage of better than 10% of a monolayer with the average K coverage measured with AES was found, substantiating the structural models.

The perfect $c(2\times2)$ structure can be formed by shifting alternate rows of Au surface atoms of the (1×2) reconstruction along [001] by one Au lattice constant. In a similar way, the $c(2\times2)$ nuclei can be formed by shifting only one row of Au surface atoms along [001]. From the shape of the $c(2\times2)$ nuclei as seen in the STM images and from the corresponding models, however, one Au atom is missing in each $c(2\times2)$ nucleus if compared with the (1×2) structure. During the nucleation of the $c(2\times2)$ phase these Au atoms must be released and presumably condense in the elevated rows. In the latter structures the density of Au atoms is increased compared

to the (1×2) reconstruction. A mass balance of Au surface atoms yields a good agreement between the number of Au atoms in the elevated rows and those missing in the $c(2\times2)$ nuclei.

The formation of $c(2\times2)$ elements can also be observed after adsorption of K at room temperature. This is demonstrated by the image reproduced in Fig. 11, where the Au(110) surface covered with ≈0.30 ML K is shown. $c(2\times2)$ stripes several hundred angstroms long are resolved. Interestingly, almost all of the (1×2) areas in Fig. 11 are in phase. Although on other surface areas K-induced APDB's were found, their concentration at room temperature was significantly smaller than after K deposition at elevated temperatures. This is attributed to kinetic restrictions. The formation of APDB's involves the shifting of entire (1×2) patches, which is apparently suppressed at room temperature. Also elevated rows are observed only scarcely. However, the possibility exists that the Au atoms released in the course of the $c(2\times2)$ formation are arranged in local (1×1) elements: In the upper right and in the lower left corner of the image in Fig. 11, areas are resolved where two $\approx$20-Å-long Au rows touch each other. These (1×1) structures are imaged ≈0.4 Å higher than the (1×2) level. The observation that the formation of the $c(2\times2)$ phase in large terraces is not kinetically limited at room temperature, as opposed to the (1×2)-(1×3) transition for lower K coverages, could be attributed to the less extensive rearrangement of substrate atoms for the formation of the $c(2\times2)$ structure. Alternatively, it might be due to an increased mobility of surface Au atoms at higher K coverages. The $c(2\times2)$ phase can also be created at room temperature by K adsorption on a regular (1×3)

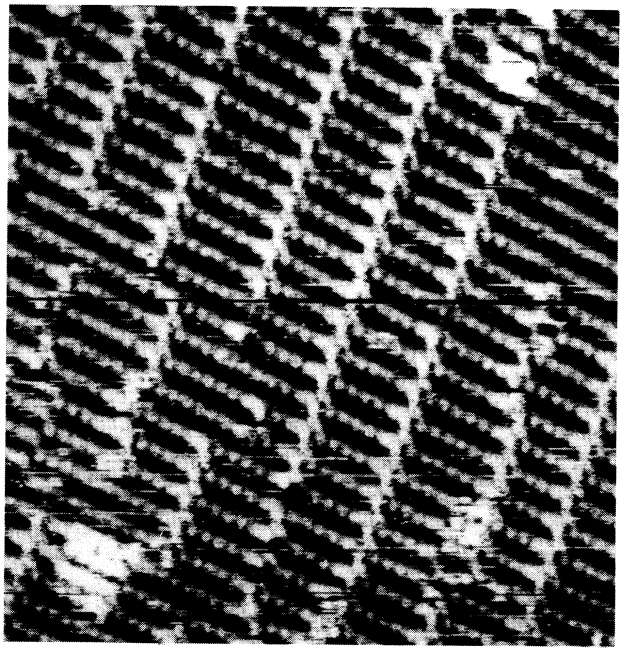

FIG. 11. Elements of the $c(2\times2)$ structure, observed after adsorption of ≈0.30 ML K at room temperature (190×190 Å^2).

FIG. 12. Lifting of the $c(2\times2)$ structure for small tunneling resistances on Au(110) with $\theta_K\approx0.35$ ML, adsorbed at $T\approx490$ K. (a) $R_t=2000$ MΩ ($U=-789$ mV, $I=0.4$ nA); (b) $R_t=30$ MΩ ($U=-489$ mV, $I=16$ nA); (c) $R_t=12$ MΩ ($U=-489$ mV, $I=40$ nA) (each 350×200 Å^2).

K/Au(110) phase with $\theta_K = 0.10$ ML, as observed by LEED. This indicates that mass transport of Au surface atoms is facilitated at higher K coverages.

Atomic-resolution images of the $c(2\times2)$ structure were difficult to achieve. This is mostly due to the fact that it becomes unstable when, in an attempt to achieve better resolution, the STM tip is brought closer to the surface (at tunneling resistances less than $\approx 100\text{M}\Omega$). This is illustrated by the series of STM images in Fig. 12: in (a) K-induced $c(2\times2)$ elements and elevated rows are resolved; after lowering the tunneling resistence in (b) a structural transition of the surface occurred. The number of $c(2\times2)$ stripes and elevated rows is reduced and (1×2) areas are resolved. Frequent fringes in the individual scan lines signal a high mobility of surface atoms during this measurement. After a further reduction of the tunneling resistance in Fig. 12(c) the surface in the scanning area is mainly (1×2) reconstructed with many APDB's. After increasing the tunneling resistance to higher values ($> \approx 100\text{M}\Omega$) the $c(2\times2)$ structures appeared again. Therefore a mass transport from adsorbed K atoms to the tunneling tip seems unlikely. Presumably, K atoms are pushed away from the area under the tip for small tunneling resistances and diffuse back after the resistance is increased again.

These tip-sample interactions are the reason why the $c(2\times2)$ structure could not be resolved for surfaces which exhibit a clear $c(2\times2)$ LEED pattern after adsorption of 0.5 ML K at elevated temperatures. In these experiments, however, additional structures were resolved which cannot be related to the $c(2\times2)$ phase, as illustrated in Fig. 13. On this surface flat areas are resolved which are associated with the $c(2\times2)$ structure. They are separated by troughs along $[1\bar{1}0]$ which are ≈ 20 Å wide and ≈ 2.5 Å deep, where presumably Au atoms of several layers are absent. These troughs are terminated in the middle of the terraces. This signals that they grow originating from the atomic steps into the terraces. The occurrence of such troughs is typical for higher K coverages, and their density increases with the adsorption temperature [the reason why the experiments for the investigation of $c(2\times2)$ formation were mostly performed for adsorption temperatures below 450 K]. Our observation agrees with MEIS results, which suggest that the saturated $c(2\times2)$ structure includes a substantial density of defects.[18]

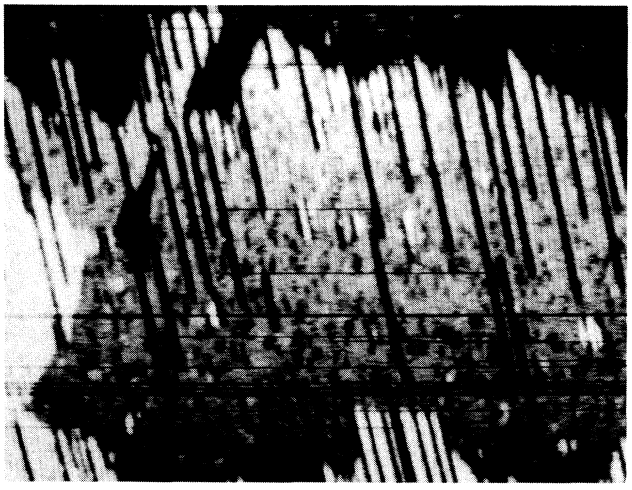

FIG. 13. Au(110) surface for a K coverage of ≈ 0.52 ML K, adsorbed at $T \approx 450$ K (1100×600 Å^2).

IV. DISCUSSION

The effects of adsorbed K atoms on the Au(110) surface can be classified into the following three regimes (for equilibrium structures):

(1) for $\theta_K < 0.15$ ML missing-row-type structures are formed which exhibit deeper furrows than the clean (1×2) reconstructed surface;

(2) in the intermediate coverage range, $0.15 < \theta_K < 0.25$ ML, the (1×2) missing-row structure of the clean Au surface is preserved; and

(3) for $\theta_K > 0.25$ ML the densely packed atomic Au rows of the substrate are disrupted and APDB's and islands of the $c(2\times2)$ reconstruction are created.

It is helpful to relate these regimes to the alkali-metal-induced work function changes. Work function data for the K/Au(110) system are not yet available. However, the changes of the work function upon alkali-metal adsorption are qualitatively the same for the various transition metals.[26,27] After a linear decrease of the work function for small coverages a minimum is reached. For higher coverages the work function increases again and approaches a value close to the work function of the pure alkali metal. For comparison, it was found for the K/Au(001) system that the work function minimum is reached at $\theta_K \approx 0.12$ ML at room temperature.[28,29] If we assume that the minimum is found for a similar density of K atoms on Au(110), the corresponding K coverage has to be ≈ 0.17 ML [the density of substrate atoms for the Au (001) and (110) planes differs by a factor of $\sqrt{2}$]. Note that the qualitative shape of the work function curve is not significantly altered if alkali-metal-induced reconstructions occur.[29–31]

With these assumptions, the (1×5) and (1×3) reconstructions are formed for coverages where the work function decreases linearly. Consequently, they occur in a coverage regime where the K-surface interaction is described by the formation of strong dipoles and where the coverage is still so small that mutual depolarization is not yet important (e.g., Ref. 32). Presumably, the driving force for the formation of the (1×5) and (1×3) structures is closely related to that of the alkali-metal-induced missing-row reconstructions on the (110) surfaces of the neighboring $3d$ and $4d$ metals Ni, Cu, Pd, and Ag.[9,11,12] All these reconstructions occur at very low coverages. We think that the driving force is a combination of surface charge transfer,[8,11] increased chemisorption energy of alkali-metal atoms in reconstruction troughs,[12] or a larger screening of the adsorbate-substrate dipoles in (deeper) missing-row furrows.

For the (1×5) and (1×3) structures the following qualitative picture is proposed. The adsorbed K atoms stabilize deep (1×3) reconstruction troughs. The effect is a local one, i.e., each K atom affects only a limited num-

ber of Au atoms in its neighborhood. This explains why, for very low coverages (around 0.05 ML), a regular (1×3) reconstruction is not formed and the balance between the repulsive interactions of the K atoms and the reconstruction energy leads to the (1×5) phase. The shape of the (1×5) unit cell, which consists of a (1×2) next to a (1×3) missing-row element, suggests that the K atoms are inhomogeneously distributed on the surface. Since the K atoms are responsible for the (1×3) furrows, we assume that they are located there and that the (1×2) troughs remain empty (cf. the model in Fig. 1). [For Pt(110) covered with ≈0.01 ML Ca, a (1×5) phase was found which similarly consists of a (1×2) and a (1×3) element.[33]]. Within the (1×3) troughs the dipole-dipole repulsion of the adatoms results in an averaged regular spacing of the K atoms. For slightly higher coverages ($\theta\approx0.08$ ML) the coverage is high enough to stabilize a regular (1×3) phase, where the K atoms are homogeneously distributed in the reconstruction channels. Hence, in our picture of the low-coverage regime, the distance between the K atoms in the (1×3) troughs is more or less constant so that, by variation of the K coverage, the amount of (1×3) reconstruction has to change. The average distance of adsorbed K atoms amounts to ≈12 Å in the (1×3) furrows of the respective reconstructions. Consequently, the influence of one K adatom is sufficient to stabilize a (1×3) element with a length of ≈12 Å on the average. The effect of the adsorbed K atoms on the Au(110) substrate is thus much larger than on a Cu(110) surface. In the latter case an adsorbed K (or Cs) atom produces a (1×2) missing-row element with an average length of only 6.3 Å (for coverages between 0.05 and 0.20 ML).[10,34]

For $\theta_K>0.1$ ML the (1×3) reconstruction is destabilized, and for $\theta_K\approx0.15$ ML the (1×2) reconstruction is the equilibrium substrate configuration. The (1×3)-(1×2) transition is in the coverage range where a nonlinear decrease of the work function is likely. This indicates that the K/substrate dipoles significantly affect each other if the average distance of K atoms in the (1×3) troughs is less than ≈10 Å. It is conceivable that the beginning of the metallization of the adlayer leads to a decrease of substrate *sp* charge density and thereby the (1×2) structure is stabilized again. Another important factor is the electrostatic energy of the K-covered surface. For a given coverage the K-K distance along $[1\bar{1}0]$ (where neighboring K dipoles are not screened by Au atoms) is smaller for the (1×3) than for the (1×2) geometry. From the destabilization of the (1×3) phase at $\theta_K\approx0.10$ ML the critical value for the interaction range of adsorbed K atoms can be estimated to be ≈10 Å. This value is in good agreement with the radius of the sphere with modified charge density for K adsorbed on Ru(0001), which was estimated to be ≈6 Å by photoemission of adsorbed Xe atoms.[35] In theoretical studies similar values were found.[36]

For $0.15<\theta_K<0.25$ ML the (1×2) missing-row structure is resolved. Therefore, unlike the (1×3) reconstruction, the average distance of the K atoms in the (1×2) troughs decreases with increasing coverage.[13,16] For $\theta_K=0.15$ and 0.25 ML these distances are 9.6 and 5.8 Å, respectively. In a similar way, K and Cs atoms which induce a (1×2) missing-row reconstruction on Cu(110) are compressed along $[1\bar{1}0]$ for coverages between 0.20 and 0.30 ML.[10,34] In these systems the K-K or Cs-Cs distance along $[1\bar{1}0]$ varies between 5.4 and 4.3 Å. By contrast, the K-K distance in the Au(110)(1×2) troughs cannot be smaller than 5.8 Å. For $\theta_K>0.25$ ML APDB's and $c(2\times2)$ structures are formed where the local K coverage is higher than in the surrounding (1×2) areas. If an atomic radius of 1.9 Å for the K atoms is assumed [corresponding to the K radius in the K/Au(110)$c(2\times2)$ configuration[17]], the distance of neighboring K atoms at an APDB amounts to 5.3 Å and hence is slightly smaller than the minimal average K-K distance in the (1×2) troughs. The electrostatic interaction energy for K/substrate dipoles with a distance of $2a$ is believed to be several tenths of an eV.[36] The energy associated with the bond between two neighboring Au atoms of an atomic row on Au(110) was estimated to be ≈0.3 eV for the clean surface[37] (using an embedded-atom method). The gain of adsorption energy of the K atoms which are bound at the ends of the interrupted Au rows and the reduction of the electrostatic repulsion must be higher than this energy (a reduction of electrostatic energy can be expected from the better screening of the K atoms at the APDB's).

The STM data presented in the previous section show the defect structure of the $c(2\times2)$ phase in the intermediate-coverage regime, where (1×2) and $c(2\times2)$ areas coexist. The $c(2\times2)$ phase was found to be arranged in highly anisotropic islands which extend usually over some ten unit cells along [001]. For example, upon deposition of 0.35 ML K at 400 K a substantial part of the surface consists of extended APDB's and $c(2\times2)$ nuclei. The anisotropy of the $c(2\times2)$ islands cannot be understood in terms of a nucleation and growth scheme: atomic motion of $c(2\times2)$ elements was observed even at room temperature, indicating a much higher mobility of the surface atoms at 400 K, corresponding to the adsorption temperature. Also, we found that upon adsorption of ≈0.08 ML K at similar temperatures the (1×2)-(1×3) transition is easily performed. Consequently, the $c(2\times2)$ defect structure represents the thermodynamic equilibrium situation.

We suggest that this defect structure can be rationalized on the basis of three different interactions: (i) an attraction between $c(2\times2)$ units along [001], (ii) very weak interactions of $c(2\times2)$ elements along $[1\bar{1}0]$, and (iii) a strong repulsion along $[1\bar{1}0]$ between K atoms adsorbed in (1×2) missing-row furrows. The attraction of the $c(2\times2)$ elements along [001] is presumably related to the different K-K and Au-Au distances in the $c(2\times2)$ geometry, which amount to 8.16 and 5.78 Å along [001] and $[1\bar{1}0]$, respectively. It does not necessarily imply a direct attraction between the K atoms at the $c(2\times2)$ sites. It can also be attributed to the energetically unfavorable termination of the $c(2\times2)$ elements along [001], resulting in a net attraction between $c(2\times2)$ unit cells. A similar effect was inferred, e.g., for K-induced missing-row elements on Cu(110).[10,38] Along the $[1\bar{1}0]$ direction such an effect does not exist. The K atoms

which terminate the $c(2\times2)$ elements in this direction and which are threefold coordinated by Au atoms are apparently not significantly disfavored against regular $c(2\times2)$ sites. The distribution of the widths of the $c(2\times2)$ strings cannot be related to strong attractive or repulsive interactions between $c(2\times2)$ elements along $[1\bar{1}0]$. There is neither an apparent tendency to form islands nor do APDB's prevail at intermediate coverages, which would indicate repulsions. A possible explanation is that there are weak attractive interactions along $[1\bar{1}0]$ but that the Au-K layer of the $c(2\times2)$ structure is under stress because of a too small lattice constant in $[1\bar{1}0]$ which prevents the formation of larger islands. Alternatively, the $c(2\times2)$ defect structure might be an entropy effect. The striking effect of the strong repulsion in $[1\bar{1}0]$ of the K atoms adsorbed in the missing-row furrows is the restriction of the lengths of the (1×2) domains (separating the $c(2\times2)$ elements in $[1\bar{1}0]$) to discrete values, leading to an in-phase arrangement of neighboring $c(2\times2)$ areas.

MEIS and theoretical studies of the K/Au(110)$c(2\times2)$ phase found that the K atoms of the $c(2\times2)$ structure are located 1.1 Å above the Au top layer.[17,18] In the STM images the positions of the K atoms of the $c(2\times2)$ areas are imaged as minima for tunneling to empty sample states at 500–1000 mV. This effect is probably not due to the mobility of the adsorbed K atoms, since they are completely surrounded by Au atoms and are therefore expected to occupy fixed positions, but to electronic imaging effects.

At large tip-sample distances and small tunneling voltages, STM images approximate contours of constant local density of states at the Fermi level of the sample.[39,40] For metallic surfaces these approximately follow the total charge density.[39] Calculations of the electronic structure of the $c(2\times2)$ shifted-row phase showed that the bonding of the surface is essentially metallic.[17] In particular, the calculations demonstrated that the charge-density contour of the surface is rather smooth and exhibits little corrugation.[17] We therefore attribute the resolution of the $c(2\times2)$ structure in the STM data to tip-surface interactions which lead to a modification of the surface electronic structure. Such interactions are also considered to be the reason for atomic-resolution images on clean close-packed metal surfaces where the charge-density corrugation of the surface is very smooth.[19,41–44] The observation that the $c(2\times2)$ phase is lifted at low tunneling resistance ($<100\text{M}\Omega$) and that resolution of the atomic structure of the $c(2\times2)$ reconstruction usually was achieved for tunneling resistance of $\approx300\text{M}\Omega$ substantiates this interpretation.

The atomic-resolution data of the $c(2\times2)$ structure show that the Au atoms in the $c(2\times2)$ areas are imaged 0.3 Å higher than the Au atoms of the surrounding (1×2) areas. Calculations and MEIS experiments both agree, however, that the relaxation of the Au surface layers is nearly identical for the clean Au(110)(1×2) and K/Au(110)$c(2\times2)$ reconstructed surfaces.[17,18] Presumably, the different imaging height of the (1×2) and $c(2\times2)$ areas is due to a different electronic structure of Au atoms in the respective areas.

V. SUMMARY

The adsorption of small amounts of K ($\theta_K<0.15$ ML) on the Au(110) surface induces a rearrangement of surface Au atoms. Structures of the missing-row type with large (111) microfacets are formed upon thermal activation. The equilibrium structure for $\theta_K\approx0.05$ and 0.08 ML is a regular (1×5) and (1×3) reconstruction, respectively. The (1×3) reconstruction consists of deep missing-row troughs where atomic Au rows of the first and second layers are missing. The (1×5) reconstruction is composed of a regular sequence of (1×3) and (1×2) missing-row troughs. For intermediate K coverages (0.15–0.25 ML) the adsorbed K atoms do not alter the (1×2) missing row reconstruction of the substrate. The K atoms are compressed in the reconstruction troughs up to an NN distance of 5.8 Å.

For $\theta_K\approx0.25$ ML the Au(110)(1×2) reconstruction is modified again. Atomic Au rows of the surface are disrupted. By shifting (1×2) areas of the terraces by one lattice constant along [001] antiphase domain boundaries for the (1×2) reconstruction are formed. For slightly higher coverages ($\theta_K\approx0.3$–0.4 ML) single [001] atomic Au rows of the surface are shifted by one lattice constant along [001], whereby elements of the $c(2\times2)$ shifted-row structure are formed. Thus, the theoretically predicted[17] shifted-row model for the $c(2\times2)$ is directly confirmed, in agreement with MEIS results for this phase.[18] The nuclei of the $c(2\times2)$ phase are identified as chains of several $c(2\times2)$ unit cells arranged along [001]. For $\theta_K>0.3$ ML antiphase domain boundaries, $c(2\times2)$ elements, and (1×2) areas coexist on the surface. The relative surface area of the $c(2\times2)$ structure increases with the K coverage. The K atoms are inhomogeneously distributed on the surface. The local K coverage is 0.5 ML at the antiphase domain boundaries and the $c(2\times2)$ elements, whereas the maximum K coverage in the (1×2) missing-row troughs is 0.25 ML. The repulsive interactions of the K atoms adsorbed in the (1×2) missing-row troughs lead to discrete lengths of the (1×2) areas along $[1\bar{1}0]$, whereby neighboring $c(2\times2)$ elements are arranged in phase.

*Present address: IBM Almaden Research Center, 650 Harry Road, San Jose, CA 95120.
†Permanent address: Institut für Oberflächenchemie und Katalyse, Universität Ulm, Albert-Einstein-Allee 11, D-89069 Ulm, Germany.

[1]W. Moritz and D. Wolf, Surf. Sci. **163**, L655 (1985).
[2]I. K. Robinson, Phys. Rev. Lett. **50**, 1145 (1983).
[3]M. Copel and T. Gustafsson, Phys. Rev. Lett. **57**, 723 (1986).
[4]P. Fery, W. Moritz, and D. Wolf, Phys. Rev. B **38**, 7275 (1988).
[5]P. Fenter and T. Gustafsson, Phys. Rev. B **38**, 10 197 (1988).
[6]G. Binning, H. Rohrer, C. Gerber, and E. Weibel, Surf. Sci. **131**, L379 (1983).
[7]M. Garofalo, E. Tosatti, and F. Ercolessi, Surf. Sci. **188**, 321 (1987).

[8]K. M. Ho and K. P. Bohnen, Phys. Rev. Lett. **59**, 1833 (1987).
[9]R. J. Behm, in *Physics and Chemistry of Alkali Metal Adsorption,* edited by H. P. Bonzel, A. M. Bradshaw, and G. Ertl (Elsevier, Amsterdam, 1989), p. 111.
[10]R. Schuster, J. V Barth, G. Ertl, and R. J. Behm, Phys. Rev. B **44**, 13 689 (1992).
[11]C. L. Fu and K. M. Ho, Phys. Rev. Lett. **63**, 1617 (1989).
[12]K. W. Jacobsen and J. K. Nørskov, Phys. Rev. Lett. **60**, 2496 (1988).
[13]D. K. Flynn-Sanders, K. D. Jamison, J. V. Barth, J. Wintterlin, P. A. Thiel, G. Ertl, and R. J. Behm, Surf. Sci. **253**, 270 (1991).
[14]P. Häberle, P. Fenter, and T. Gustafsson, Phys. Rev. B **39**, 5810 (1989).
[15]B. M. Ocko, G. Helgesen, B. Schardt, J. Wang, and A. Hamelin, Phys. Rev. Lett. **69**, 3350 (1992).
[16]R. J. Behm, D. K. Flynn, K. D. Jamison, G. Ertl, and P. A. Thiel, Phys. Rev. B **36**, 9267 (1987).
[17]K. M. Ho, C. T. Chan, and K. P. Bohnen, Phys. Rev. B **40**, 9978 (1989).
[18]P. Häberle and T. Gustafsson, Phys. Rev. B **40**, 8218 (1989).
[19]J. Wintterlin, J. Wiechers, H. Brune, T. Gritsch, H. Höfer, and R. J. Behm, Phys. Rev. Lett. **62**, 59 (1989).
[20]H. Brune, J. Wintterlin, J. Trost, G. Ertl, J. Wiechers, and R. J. Behm, J. Chem. Phys. **99**, 2128 (1993).
[21]G. Doyen, D. Drakova, J. V. Barth, R. Schuster, T. Gritsch, R. J. Behm, and G. Ertl, Phys. Rev. B **48**, 1738 (1993).
[22]T. Gritsch, D. Coulman, R. J. Behm, and G. Ertl, Surf. Sci. **257**, 297 (1991).
[23]J. K. Gimzewski, R. Berndt, and B. R. Schlittler, Phys. Rev. B **45**, 6844 (1992).
[24]C. J. Raub and V. B. Compton, Z. Anorg. Chem. **332**, 5 (1964).
[25]K. J. Range, F. Rau, and U. Klement, Acta Crystallogr. Sec. C **44**, 1486 (1988).
[26]T. Aruga and Y. Murata, Prog. Surf. Sci. **31**, 61 (1989).
[27]K. Wandelt, in *Physics and Chemistry of Alkali Metal Adsorption* (Ref. 9) p. 25.
[28]S. Schröder, Diploma thesis, FU Berlin, 1991.
[29]M. Okada, H. Iwai, R. Klauser, and Y. Murata, J. Phys. Condens. Matter **4**, L593 (1992).
[30]R. Döhl-Oelze, E. M. Stuve, and J. K. Sass, Solid State Commun. **57**, 323 (1986).
[31]M. Okada, H. Tochihara, and Y. Murata, Surf. Sci. **245**, 380 (1991).
[32]B. N. J. Persson and H. Ishida, Phys. Rev. B **42**, 3171 (1990).
[33]M. Stock, J. Risse, U. Korte, and G. Meyer-Ehmsen, Surf. Sci. **233**, L243 (1990).
[34]R. Schuster, Ph.D. thesis, FU Berlin, 1992.
[35]K. Markert and K. Wandelt, Surf. Sci. **159**, 24 (1985).
[36]N. D. Lang, S. Holloway, and J. K. Nørskov, Surf. Sci. **150**, 24 (1985).
[37]L. D. Roelofs, S. M. Foiles, M. S. Daw, and M. I. Baskes, Surf. Sci. **234**, 63 (1990).
[38]R. Schuster, J. V. Barth, G. Ertl, and R. J. Behm, Surf. Sci. Lett. **247**, L229 (1991).
[39]J. Tersoff and D. R. Hamann, Phys. Rev. B **31**, 805 (1985).
[40]N. D. Lang, Phys. Rev. Lett. **56**, 1164 (1986).
[41]S. Ciraci, A. Baratoff, and I. P. Batra, Phys. Rev. B **42**, 7618 (1990).
[42]G. Doyen, E. Koetter, J. Barth, and D. Drakova, in *Basic Concepts and Applications of Scanning Tunneling Microscopy,* edited by R. J. Behm, N. Garcia, and H. Rohrer (Kluwer, Dordrecht, 1990), p. 97.
[43]G. Doyen, E. Koetter, J. P. Vigneron, and M. Scheffler, Appl. Phys. A **51**, 281 (1990).
[44]E. Tekman and S. Ciraci, Phys. Rev. B **42**, 1860 (1990).

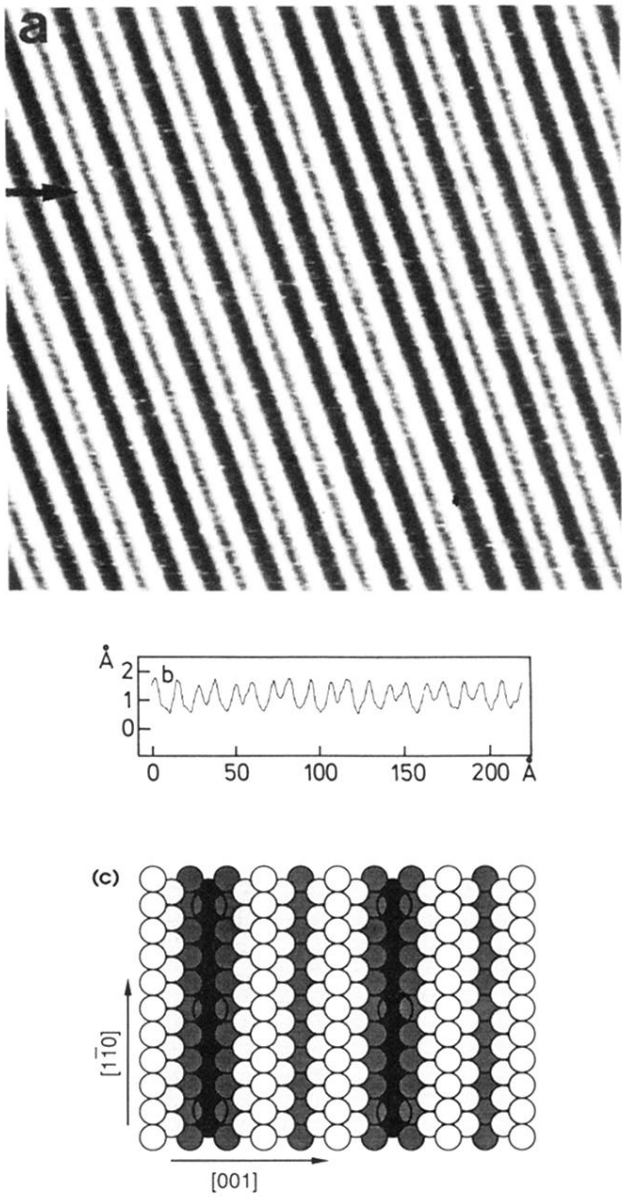

FIG. 1. (a) STM image of the Au(110) surface for $\theta_K \approx 0.05$ ML (annealed to 1000 K). Domains of the K-induced (1×5) reconstruction separated by single (1×3) elements are resolved (220×220 Å^2); (b) contour line along the marked direction in (a) (arrow); (c) model of the K-induced (1×5) reconstruction; small circles correspond to Au atoms, lower-lying atoms are darker colored, and large open circles correspond to adsorbed K atoms.

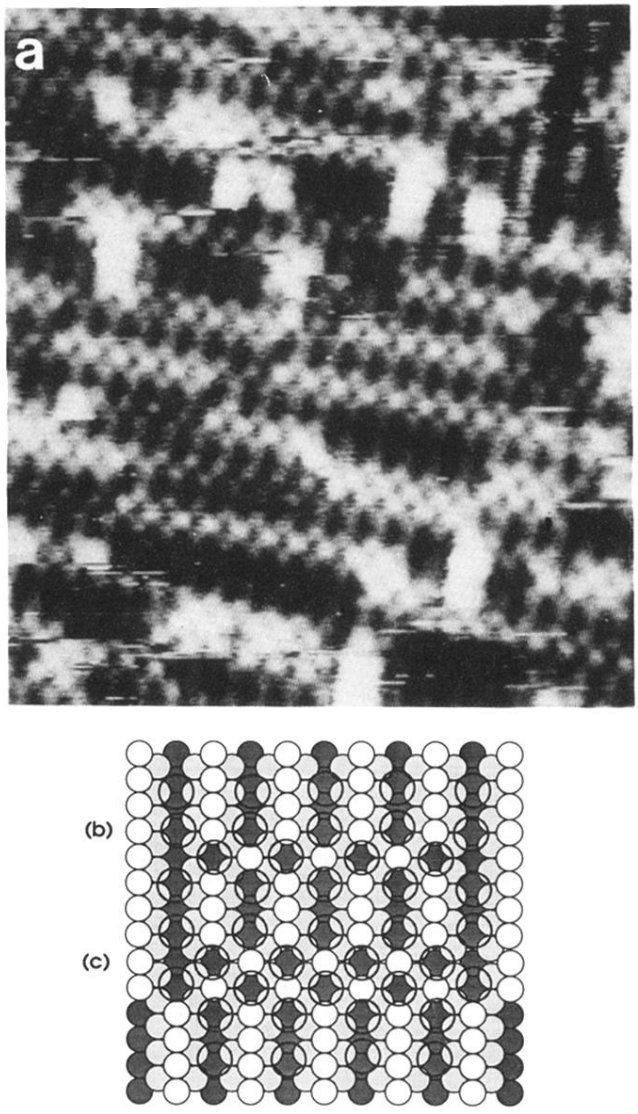

FIG. 10. (a) Atomic-resolution STM image of the K-induced structures on Au(110) for $\theta_K \approx 0.35$ ML, adsorbed at $T \approx 400$ K (170×180 Å^2); (b) model for the $c(2\times2)$ nucleus; (c) model for the $c(2\times2)$ antiphase domain boundary.

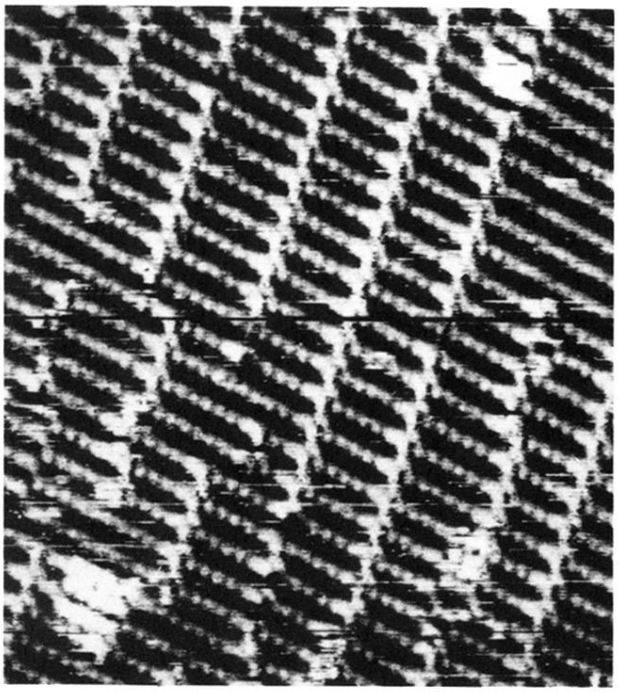

FIG. 11. Elements of the $c(2\times2)$ structure, observed after adsorption of ≈ 0.30 ML K at room temperature (190×190 Å^2).

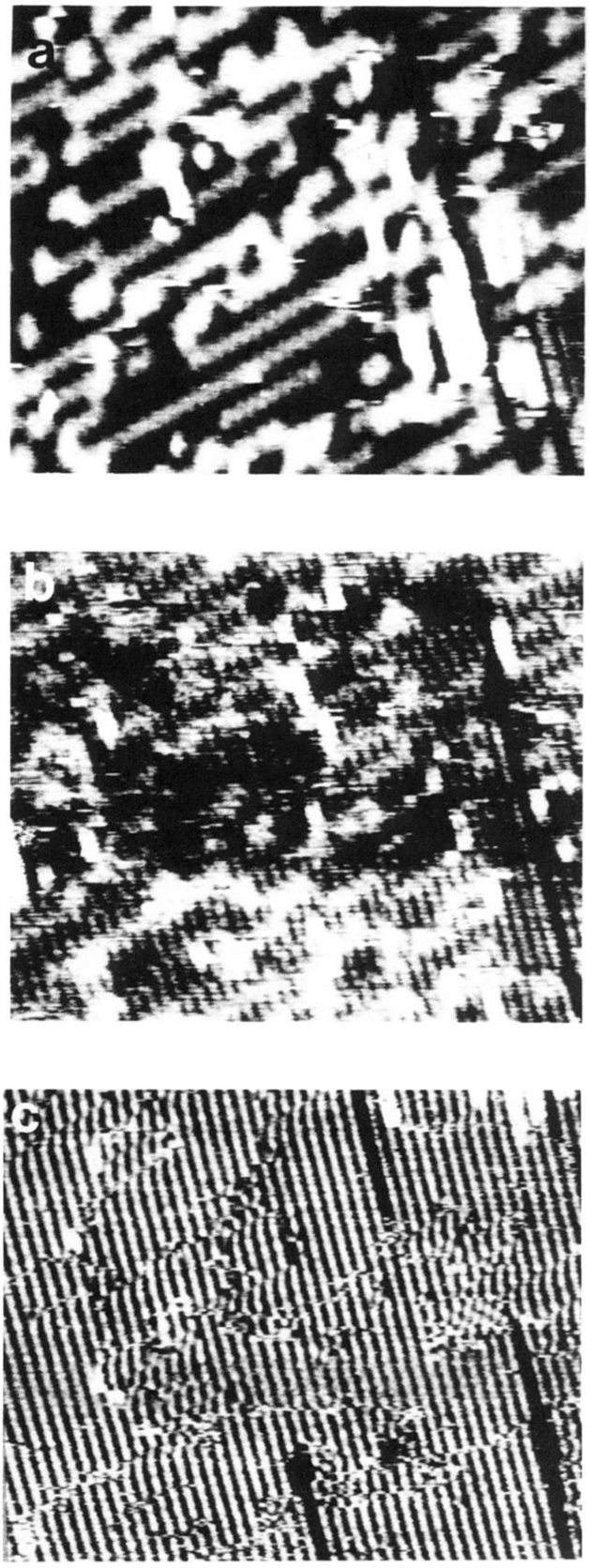

FIG. 12. Lifting of the $c(2\times2)$ structure for small tunneling resistances on Au(110) with $\theta_K \approx 0.35$ ML, adsorbed at $T \approx 490$ K. (a) $R_t = 2000$ MΩ ($U = -789$ mV, $I = 0.4$ nA); (b) $R_t = 30$ MΩ ($U = -489$ mV, $I = 16$ nA); (c) $R_t = 12$ MΩ ($U = -489$ mV, $I = 40$ nA) (each 350×200 Å^2).

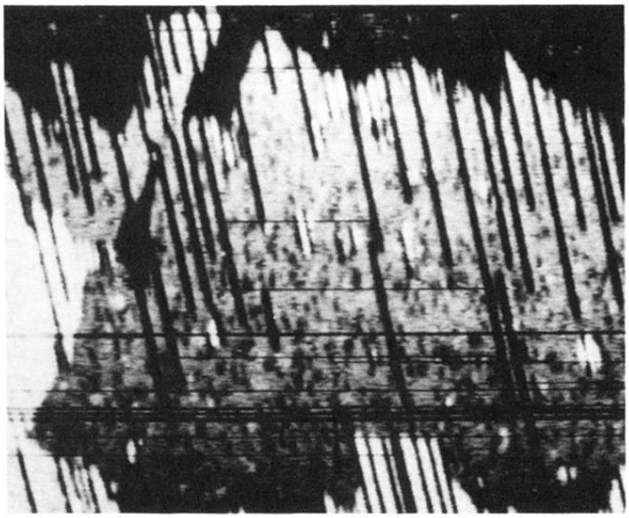

FIG. 13. Au(110) surface for a K coverage of ≈ 0.52 ML K, adsorbed at $T \approx 450$ K (1100×600 Å^2).

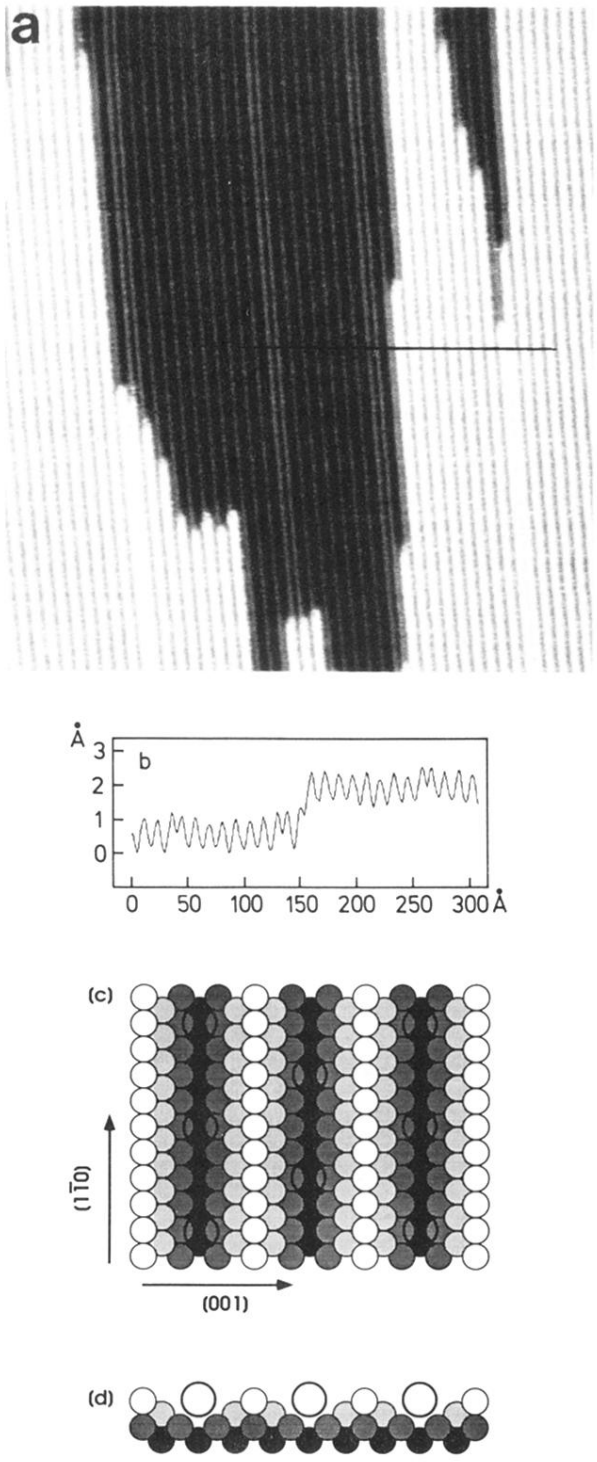

FIG. 2. (a) STM image of the Au(110) surface for $\theta_K \approx 0.08$ ML (annealed to 950 K): K-induced (1×3) reconstruction with single (1×2) troughs (610×510 Å^2); (b) STM contour along the marked line in (a); (c) model of the K-induced (1×3) phase on Au(110), top view; (d) side view.

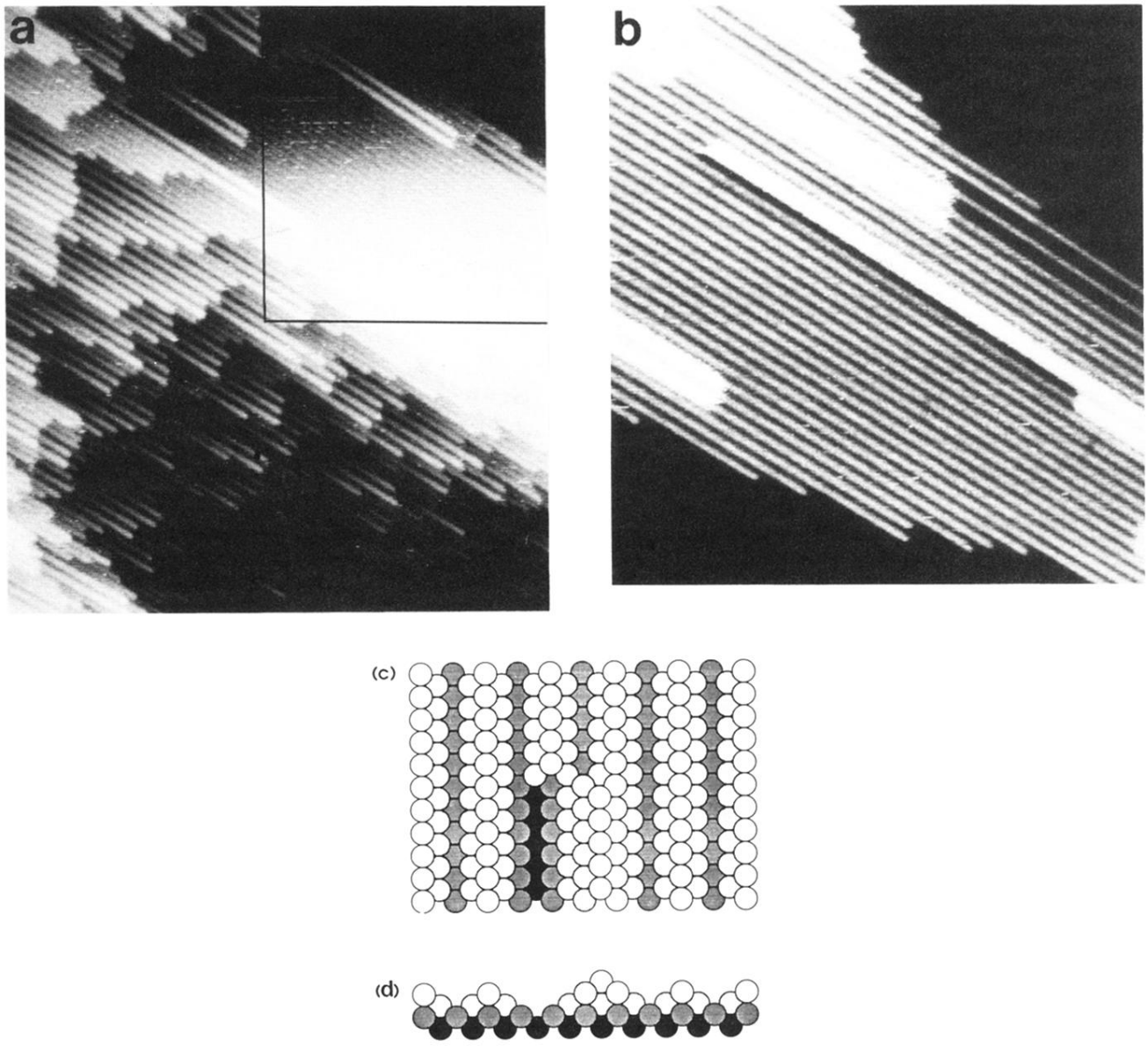

FIG. 3. Au(110) surface ≈30 min after the adsorption of ≈0.08 ML K at room temperature (700×700 Å^2); (b) detail from the area marked in (a), recorded ≈5 min later (370×370 Å^2). Model of the elevated row: (c) top view; (d) side view.

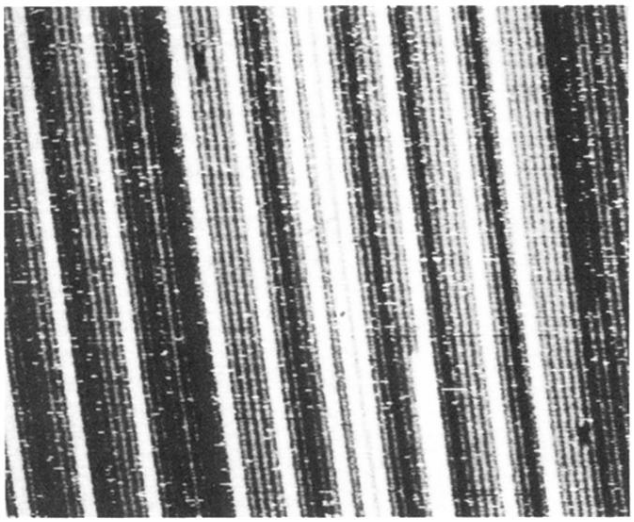

FIG. 4. Au(110) for $\theta_K \approx 0.10$ ML adsorbed at $T \approx 450$ K (570×450 Å^2).

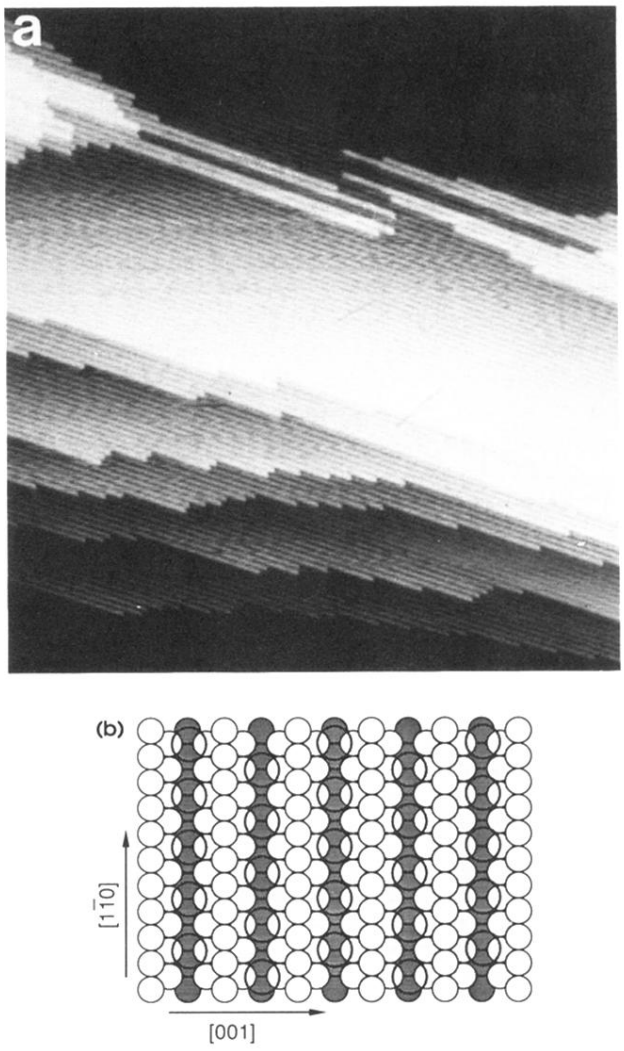

FIG. 5. Au(110)(1×2) missing-row reconstruction for $\theta_K \approx 0.15$ ML K, adsorbed at 700 K (900×900 Å^2); (b) model of the K-covered (1×2) reconstruction with $\theta_K = 0.25$ ML.

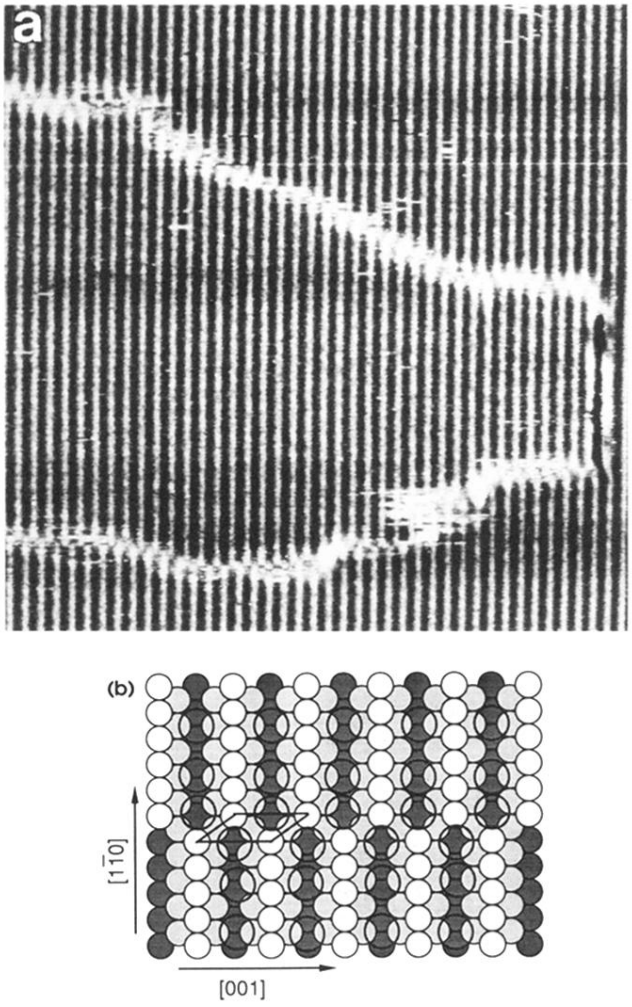

FIG. 6. Au(110) for $\theta_K \approx 0.25$ ML K, adsorbed at $T \approx 450$ K. (a) Antiphase domain boundaries of the (1×2) reconstruction (370×370 Å^2); (b) model of the K-induced antiphase domain boundary at $\theta_K \approx 0.25$ ML.

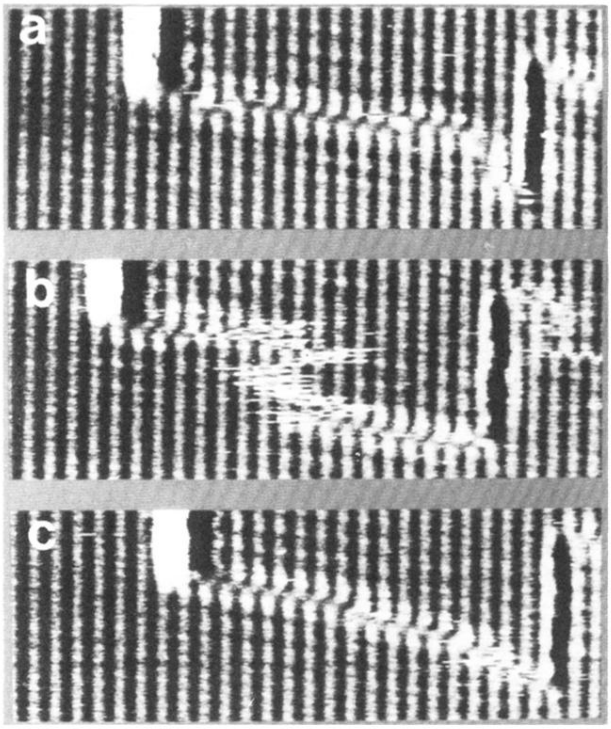

FIG. 7. Mobility of the antiphase domain boundaries for $\theta_K \approx 0.25$ ML, adsorbed at $T \approx 450$ K. The images in (b) and (c) were recorded ≈ 5 and 10 min after the image in (a), respectively (each 230×80 Å^2).

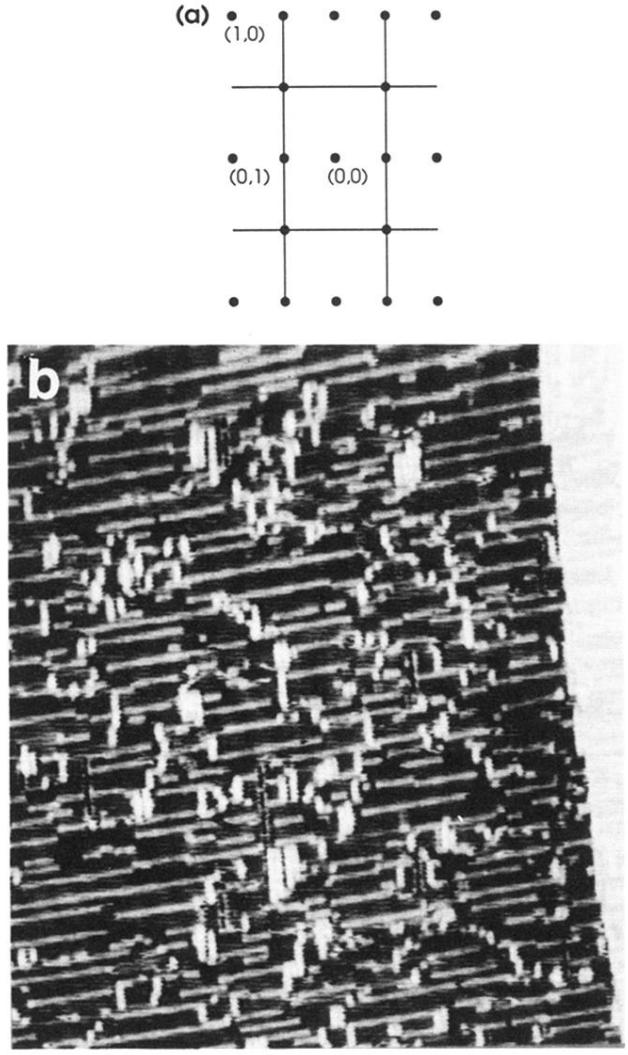

FIG. 8. (a) Schematic LEED pattern of the Au(110) surface covered with 0.30–0.35 ML, K, adsorbed at ≈ 400 K; (b) corresponding STM image ($\theta_K \approx 0.30$ ML; 1000×1000 Å^2).

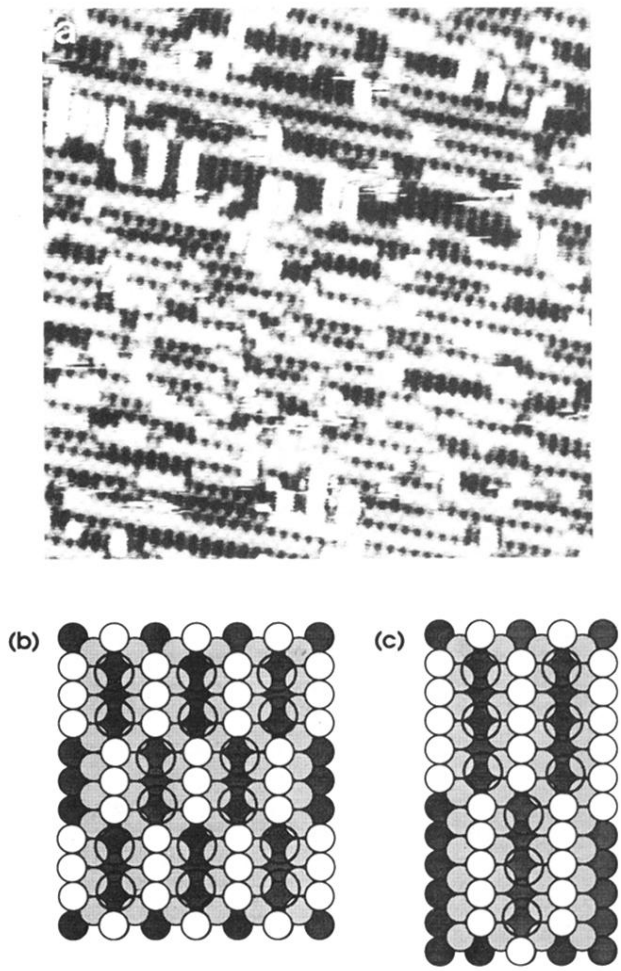

FIG. 9. (a) Au(110) for $\theta_K \approx 0.35$ ML, adsorbed at $T \approx 400$ K (350×350 Å^2). (b) K-induced antiphase domain boundaries regular network with a periodicity of $3a$ along $[1\bar{1}0]$; (c) three K atoms fit into a (1×2) trough with a length of $5a$.